Science and Technology for the Built Environment

ISSN: 2374-4731 (Print) 2374-474X (Online) Journal homepage: http://www.tandfonline.com/loi/uhvc21

A comparison of numerical simulation methods analyzing the performance of a ground-coupled heat pump system

Angelo Zarrella, Roberto Zecchin, Philippe Pasquier, Diego Guzzon, Michele De Carli, Giuseppe Emmi & Michele Quaggia

To cite this article: Angelo Zarrella, Roberto Zecchin, Philippe Pasquier, Diego Guzzon, Michele De Carli, Giuseppe Emmi & Michele Quaggia (2018): A comparison of numerical simulation methods analyzing the performance of a ground-coupled heat pump system, Science and Technology for the Built Environment, DOI: 10.1080/23744731.2018.1438663

To link to this article: https://doi.org/10.1080/23744731.2018.1438663

Accepted author version posted online: 01 Mar 2018.

Publisher: Taylor & Francis

Journal: *Science and Technology for the Built Environment*

DOI: https://doi.org/10.1080/23744731.2018.1438663

A comparison of numerical simulation methods analyzing the performance of a ground-coupled heat pump system

ANGELO ZARRELLA[1*], ROBERTO ZECCHIN[2,3], PHILIPPE PASQUIER[4], DIEGO GUZZON[3], MICHELE DE CARLI[1], GIUSEPPE EMMI[1], MICHELE QUAGGIA[3]

[1]Department of Industrial Engineering – Applied Physics Section, University of Padova, Via Venezia 1 – 35131, Italy

[2]University of Padova, Via VIII Febbraio 2 – 35122, Italy

[3]Manens-Tifs S.p.A., Padova, Corso Stati Uniti 56 – 35127, Italy

[4]Department of Civil, Geological and Mining Engineering, Polytechnique Montréal, P.O. Box 6079, Centre-Ville, Montreal, H3 C 3A7, Canada

[*]Corresponding author email: angelo.zarrella@unipd.it

Ground-coupled heat pumps are increasingly being utilized to heat and cool buildings. Although it is difficult to size and to predict their behaviour and performance, their design can be optimized via simulations. EnergyPlus is a popular energy simulation program for modeling building heating and other energy flows and, since it is organized to consider borehole heat exchangers via the well-known g-functions approach, it can be used advantageously for that purpose. CaRM is another recent numerical simulation tool devoted to ground and borehole heat exchangers. In this work, two methods to calculate the g-fucntions were analyzed, using as case-study a real office building, whose imbalance between the heat extracted and injected into the ground was found to be appreciable. The energy imbalance involves a ground temperature drift affecting the system efficiency. The results of the EnergyPlus g-functions and the CaRM model approaches were compared. The capacity of the two methodologies to accurately simulate this phenomenon were analysed also with reference to the available building's long-term monitoring data. The analysis showed the importance of using g-functions suitable to reflect the layout of the borehole field, in order to correctly evaluate the energy performance of the entire ground source heat pump system.

Keywords

Ground source heat pump systems, Ground heat exchanger, Borehole, G-functions, EnergyPlus.

Introduction

It is well known that energy use in buildings is one of the most important challenges facing sustainable development. In this regard improving efficiency and reducing demands are widely considered the most promising, easiest, quickest, and safest means to mitigate climate changes (Ürge-Vorsatz et al. 2015; Sorrell, 2015).

The building sector is responsible for approximately 40% of energy consumption and 36% of CO_2 emissions in Europe (European Parliament, 2016). The 2010 edition of the Energy Performance of Buildings Directive (EPBD) (European Parliament, 2010) and the 2012 Energy Efficiency Directive (EED) (European Parliament, 2012) are legislative acts aiming to shape Europe's measures to attain its goals of improving buildings' energy efficiency. These measures are needed also given the poor energy efficiency conditions of many existing buildings leading to high energy consumption. The building sector has been the object of several energy efficiency policy recommendations over the past ten years. The EPBD is being implemented and beginning to show its first effects. At the same time, the International Energy Agency-IEA (IEA 2011, 2016) has defined energy efficiency of buildings as one of the measures that can be utilized to secure long-term decarbonisation of the energy sector. In this context, heat pump technology could play a key role in improving energy efficiency and in reducing fossil fuel consumption by exploiting low-temperature heat sources not otherwise directly available for space heating and domestic hot water (DHW) production. In 2015, about 26% of the total heat generated in Italy from renewable sources and consumed in direct ways by families and enterprises was obtained through heat pumps (GSE, Gestore dei Servizi Energetici, 2017). This value was calculated according to the Directive 2009/28/EC (European Parliament, 2009) taking into account the heating mode of heat pumps only; the air and ground source heat pumps contribute to that value for about 97% and 3%, respectively. However, according to GSE (GSE, Gestore dei Servizi Energetici, 2017), it is to be cosidered that the direct use of heat from renewable sources is measured only on large plant-systems, in other cases the evaluation is based on set of samples and market data.

The scientific community has been working diligently over the past decades to identify measures that could improve the energy efficiency of entire buildings and to exploit renewable energy sources. Many studies have been conducted to examine the most efficient cost-effective building envelopes and plant system measures. Three main categories have been identified for this purpose: planning and designing strategies, the building envelope including the material and equipment utilized, and the technologies for the energy generation and for the renewable energy exploitation. At the same time, as some investigators have pointed out, the best way to enhance energy efficiency is to maximize reliance on passive systems while minimizing use of active ones (Al-Sallal, 2014).

Algoritms for building energy analysis have come quite a distance since they first began to be developed in the sixties (Stephenson and Mitalas, 1967), and efficient simulation models have been available since the seventies. Among these, the National Bureau of Standards Load Determination (NBSLD), which was developed by Kusuda (1976), provided novel features based on the detailed solution of simultaneous heat balance equations at all of the interior surfaces of a room or space and through the exterior walls. Further experience generated by other undertakings such as DOE-2 and BLAST subsequently led to EnergyPlus (U.S. Department Of Energy, 2016), a notable computer simulation software widely used for design analysis and certification procedures, e.g. LEED (U.S.

Green Building Council, 2017). The whole energy simulation program enables to analyse building characteristics and heating, ventilating, and air-conditioning (HVAC) system responses.

Although one of such systems, the borehole ground-coupled heat pump, has been receiving considerable attention, it is difficult to analyse a borehole field because of the complexity of bore field geometry and the impact of ground thermal properties. Relatively simple conduction transfer functions were thus adopted within the EnergyPlus program to model the borehole heat exchangers (BHE) and to evaluate fluid temperatures and relevant energy fluxes. The complex thermal interactions between the boreholes, when this approach is used, are evaluated via so-called g-functions, a concept introduced by Eskilson a few decades ago (Eskilson, 1987). The downloadable version of EnergyPlus includes precomputed g-functions for three borehole field configurations, namely 1×2, 4×4 and 8×8 regular grids, with 4.6 m spacing and a grout thermal conductivity of 0.74 or 1.47W/(m K). The representativeness of the model drops dramatically when BHE characteristics differ from default ones.

A site-specific fitting of g-functions requires an external computer code, such as the one implemented in the GLHEPro software (Spitler, 2000) and outlined in the EnergyPlus handbook. The latest GLHEPro version implements the simulation of the whole ground source heat pump system. The characteristics of the borehole field can be specified to allow one-hour time step simualtions via the EnergyPlus software. For vertical BHEs, the long-time step (LTS) g-functions developed by Eskilson (Eskilson, 1987) with a finite difference model are used and a database of 307 precomputed g-functions is included with the GLHEPro. For short-time steps (STS), Yavuzturk et al. (1999) numerically solved a transient heat diffusion problem with a 2D model taking into account the borehole geometry (borehole and pipe radius, pipe spacing, etc.) as well as the thermal conductivity and the capacity of the grout and pipe containing the heat carrier fluid. The method was later improved by Xu and Spitler (2006) who reduced the computation time.

Over the past few years, several studies have been carried out to construct LTS g-functions for various boundary conditions along the borehole wall (Cimmino and Bernier, 2014; Priarore and Fossa, 2016), in the case of arbitrarily inclined boreholes (Cui et al., 2006; Marcotte and Pasquier, 2009; Lamarche, 2011; Lazzarotto, 2016; Lazzarotto and Bjork, 2016), for boreholes connected in parallel or mixed arrangements (Lazzarotto, 2014; Marcotte and Pasquier, 2014), with different inlet conditions (Lamarche, 2017) and also considering the vertical heat flux at the surface level of the ground (Rivera et al. 2016 a, 2016b, 2017). Nowdays, the most common approach consists in linearly combining the unit response of the finite-line source model (FLS) (Zeng et al., 2002; Lamarche and Beauchamp, 2007; Marcotte et al., 2010; Claesson and Javed, 2011) to generate LTS g-functions.

The g-function concept is relatively easy to implement and expresses the complex thermal interactions within the BHE using a single smooth function. The g-function, however, presupposes a steady-state heat transfer within the borehole and neglects the thermal capacity of the grout, fluid and pipe that control the short-time behaviour of the inlet temperature and the heat pump operation. In some applications, short time simulations of ground-coupled systems are needed, especially when intermittent heat pump operations are involved. Although recent techniques have been proposed to construct a transfer function simultaneously registering the STS and LTS of the outlet fluid temperature (Pasquier and Marcotte, 2014; Ruiz-Calvo et al., 2016), for the moment they are limited to a single borehole.

As an alternative to the solutions mentioned above, it is possible to simulate the behaviour of a geothermal field by resorting to numerical approaches such as finite difference, finite element, or finite volume models. Although these methods require longer computational times, they describe the field perfectly as they represent a direct application of Fourier's law and at the same time consider the thermal capacity of the grouting material, pipes and the one of heat carrier fluid. One of these methods is the CaRM (CApacity Resistance Model) (Zarrella et al., 2013 a). The entire ground source heat pump system (i.e. both the heat pump and the borehole heat exchangers) can be simulated via the model's latest version (Zarrella et al., 2013b). Simulating the performance of a GSHP system can be useful both at the design stage and to analyse the thermal behaviour of a given borehole field. The borehole field of each building requires a specific design because it has a different impact on the entire building-plant system. A GSHP system simulation should also accurately analyse the real effect of different characteristics, e.g. long time and low amplitude or short-time and high amplitude.

The current study is set out to compare the results obtained from analytical g-functions and the finite difference algorithm CaRM. The comparison consists in a long-term hourly analysis of heating and cooling loads of a real office building, located in Italy, characterised by an appreciable imbalance between the energy exchanged with the ground in the summer as well as in the winter. The present study outlines the importance to calculate the g-functions according to the real layout of the borehole field and also how this can affect the thermal bahavior on the long term.

Method

The g-functions

In his pioneering work on g-functions, Eskilson (1987) used a transient finite difference model with a uniform, constant temperature along the borehole wall and the superposition principle to construct a dimensionless function linking the borehole wall temperature and the extraction rate over the BHE. Given the dimensionless nature of the g-function, it is possible to precompute the transfer function and apply it to various BHE configurations and ground thermal properties.

Once constructed, the g-function of the BHE is convoluted with the incremental heat flux signal to obtain the mean fluid temperature in accordance with the equation below:

$$T_f(\tau) = T_g + q(\tau) \cdot R_b + \sum_{i=1}^{n} \left(\frac{q_i - q_{i-1}}{2\pi \cdot \lambda} \cdot g\left(\frac{\tau - \tau_{i-1}}{\tau_s}, \frac{r_b}{L_{bore}} \right) \right) \quad (1)$$

where $\tau_s = L_{bore}^2 / (9 a_g)$ is the characteristic time.

Eskilson's original work considered the situation of a uniform temperature along the borehole wall that was the same for all the boreholes present in the field. To explain the influence of the boundary conditions on early time steps, Eskilson proposed using a constant heat extraction–injection rate on the time-scale below:

$$\tau = \frac{5 r_b^2}{a_g} \quad (2)$$

This time step for a typical borehole can last between 2 to 6 hours.

Cimmino et al. (2013) recently considered the case of a uniform heat flux along the height of a borehole wall to construct a g-function with a mean wall temperature that was the same for all the boreholes. Based on the finite line source (FLS) model, the approach considers the buried depth of the borehole head and has been implemented in a standalone toolbox Cimmino and Bernier (2013) that is available upon request. Its availability, ease of use and capacity to handle irregular layout of BHEs led us to choose it to carry out this study.

The CaRM approach

The CaRM tool solves Fourier's equation of the thermal field numerically using the electrical analogy; the most recent version of the CaRM (Zarrella and Pasquier, 2015; Zarrella et al., 2013 a) constitutes an important step forward with respect to earlier ones (De Carli et al., 2010). The borehole heat exchanger and the ground are discretized with thermal nodes upon which the heat balance equations are based. The most recent version (Zarrella and Pasquier, 2015; Zarrella et al., 2013 a) calculates the heat exchange between the heat-carrier fluid inside the boreholes and the surrounding ground and considers also the axial heat conduction within both the grout and the ground. Convective heat transfer and the short-long wave radiation exchange at the ground surface are also modelled but the moisture movevent and latent heat transfer are not considered (Kollet et al., 2009). This approach makes it possible to analyse short borehole heat exchangers that are generally utilized in situations in which the ground temperature is affected by near-surface effects. The model also considers the shape of the borehole field. Figure 1 outlines the CaRM approach.

The model resorts to thermal resistances and capacitances in order to solve the unsteady state heat transfer problem. The ground is divided into three main zones: the immediate surface, the borehole, and the deep zones (Figure 1.a). The heat transfer model adopted varies depending upon the zone being considered: one-dimensional heat conduction (i.e. along the depth direction) is modelled at both the surface and deep zones. Heat transfer takes place in the radial and axial directions in the intermediate borehole zone. The energy balance is calculated for each thermal node (Figure 1.b-c) of the domain. The CaRM tool can investigate a variety of borehole heat exchangers: single and double U-tube, coaxial pipes, helical shaped pipe and energy piles whose characteristics do not conform to the g-functions application outlined above and require a specific analysis (Zarrella et al., 2017). The building load profile is required for CaRM simulation; the tool calculates the ground temperatures and the inlet and outlet heat-carrier fluid temperatures along the boreholes at each simulation time step.

The case study

The edifice used for the current study, a four-storey office building with a total floor area of 2,200 m^2 is located in the city of Padova (Italy). Three of the floors are above ground and one is underground (Figure 2.a). Approximately 90 people work in the building on week days. The North and South facades are completely glazed (the South one is a double-skin type). The west-side wall is opaque with a large central window on the first two floors; the top floor of the west-side is fully glazed. Construction was completed in 2003, and the entire building has been operational since 2004. Thermally activated radiant and primary air HVAC systems were installed: the air

handling unit is switched on during the day time and the thermally activated radiant building system during the night time (Currò Dossi et al., 2003). This strategy reduces the building's peak load.

The building's heating and cooling demands are fulfilled by a 4-step water to water heat pump coupled to the ground via 16 boreholes. The boreholes, which are 95 m long and 7 m apart, are arranged in an L-shape pattern (Figure 2.b). The heat pump, which runs with refrigerant R407 C, is used for both space heating and cooling; its nominal capacity is 111 kW and 97 kW in cooling and heating modes, respectively. The heat pump operates with one temperature set-point in the heating mode (35 °C) and two in the cooling mode, (7 °C in the day time for the dehumidification of the primary air and 17 °C during the night time for the thermally actived radiant building system) to improve the energy efficiency when no air handling is required. The main characteristics of the heat pump are outlined in Table 1.

The borehole's collecting circuit is buried about 1 m beneath the ground surface. A double U-tube heat exchanger with high density polyethylene pipes was installed inside the borehole. The outer and inner diameters of the pipe are 32 and 26 mm, respectively; the borehole diameter is 140 mm. The two loops of the double U-tube and all the boreholes of the field are positioned in a parallel arrangement. The heat-carrier fluid inside the ground heat exchanger, which is pure water, has a total constant mass flow rate equal to 5.56 kg/s.

On the building side of the heat pump, the total mass flow rate of the heat-carrier fluid is equal to 6.10 kg/s. The fluid mass flow rates in the loops were considered constant throughout the simulation time and in active mode depending on the schedule and requirement of the heat pump.

As no thermal response tests were carried out before the BHEs were constructed, the ground properties were predicted on the basis of geological samples obtained during the drilling operations. The simulations were carried out analysing the mean thermal properties (i.e. thermal conductivity, density and specific heat capacity) calculated as a weighted average of the properties over the layer thickness. This approach does not lead to noticeable errors in the simulation outcome (Luo et al., 2014). The mean weighted thermal conductivity was assumed to be 1.9 W/(m K) and the volumetric heat capacity 2.24 MJ/(m^{3}K). The undisturbed ground temperature was estimated to be 14 °C (annual mean external air temperature at the location). Given the location's characteristics, the local groundwater flow was considered negligible.

The building's hourly heating and cooling demands were calculated over an eleven year period, i.e. between 2005 and 2015 using EnergyPlus software. Real weather data was provided by the Regional Agency for Environmental Protection (ARPAV, 2017) collected at the weather station of the village of Legnaro, which is located about ten kilometres away from the building, the area being flat country.

The EnergyPlus energy model was developed dividing the whole building into 59 thermal zones, each with its own geometry, glazed and solar shading surfaces. The thermal properties of the opaque walls were calculated, and the internal heat gains were set for each zone. The air handling unit and the thermally activated building system were modelled in EnergyPlus as well.

OpenStudio software, which uses the EnergyPlus computing engine, was utilized to create the external surfaces and internal partitions of the building, taking into account the thermophysical properties of each material. Table 2 shows the resulting transmittance of the external surfaces. The above-ground window-wall ratio is about 67%. An

automatic shading system, including blinds located between the two glass layers of the double skin facade, is controlled by the global incident solar radiation on the window; if the solar radiation exceeds the 200 W/m^2 set-point, the shade control is activated. The glazing facade on the north side of the building has a manual interior shading device to minimize glare.

The thermal loads (lights, occupancy and electric equipment) in each thermal zone were carefully examined to calculate their maximum values and to create real operating conditions. The load schedules of the internal loads and occupancy reflect typical patterns from 8:00 to 18:00. There are also daylight occupancy sensors in all the zones that also consider the contribution of natural light to maintain a 500 lux lighting level at the desks. Table 3 summarizes relevant data regarding different internal areas.

The air handling unit and the thermally activated building system were simulated with EnergyPlus. The minimum air handling unit design flow rate is approximately 7000 m^3/h, i.e. the average outdoor air flow rate value for the entire building is approximately 1 vol/h. The thermally activated building system was also modelled in EnergyPlus considering the actual stratigraphy of the radiant surface and the high thermal inertia of the system.

The ground source heat pump was also modelled with EnergyPlus. The efficiency and performance curves of the equipment required by EnergyPlus were obtained from technical documents supplied by the manufacturer for different operating conditions.

Each simulated year was split into the winter (from October 15th to April 15th) and summer seasons (from April 16th to October 14th), as indicated in national regulations. The indoor temperature set-point during the winter was 21 °C; it was 24 °C during the summer. The flow chart in Figure 3 shows the steps to develop the model.

Figure 4 shows the thermal loads of the building, in this case the heat pump was well-sized, consequenlty all building loads are satisfied during the year. The ratio between the annual heating and cooling energy demands ranges from 0.6 initially to 0.5 at the end of the eleven year period. This confirms that the building's annual load profile is cooling dominant.

The building is equipped with a BMS (Building Management System) that measures and stores not only the data concerning the control of the HVAC system but also those concerning the overall behaviour of the building-plant system; this was done specifically for research purposes.

Computer simulations

The three simulation approaches that were used and compared were:

- *Method 1*: the building and ground source heat pump were simulated jointly in EnergyPlus using g-functions calculated via GHLEPro (Spitler, 2000);
- *Method 2*: the same method as in 1, but the g-functions were calculated using the tool generated by Cimmino and Bernier (2013);
- *Method 3*: the building was simulated in EnergyPlus and the ground source heat pump was successively analysed via the CaRM tool, starting from the thermal loads previously calculated for methods 1 and 2.

In addition to the real layout of the borehole field of the building studied here, two other configurations were examined to make the comparison more complete. In all the layouts considered, the total borehole length was

maintained constant and only the position of the boreholes was modified. Table 4 describes the three cases investigated.

At each time step, the energy efficiency of the heat pump was calculated according to the following equations in the cooling mode:

$$\frac{Q_c}{Q_{c,nom}} = -0.25 + 7.3574\left(\frac{T_{L,in}}{T_{ref}}\right) - 2.3973\left(\frac{T_{S,in}}{T_{ref}}\right) - 1.5156\left(\frac{\dot{V}_L}{\dot{V}_{nom}}\right) - 2.25\left(\frac{\dot{V}_S}{\dot{V}_{nom}}\right) \quad (3)$$

$$\frac{P_{elc}}{P_{elc,nom}} = 0.5625 + 1.4518\left(\frac{T_{L,in}}{T_{ref}}\right) + 5.9483\left(\frac{T_{S,in}}{T_{ref}}\right) - 3.125\left(\frac{\dot{V}_L}{\dot{V}_{nom}}\right) - 4.125\left(\frac{\dot{V}_S}{\dot{V}_{nom}}\right) \quad (4)$$

where T_{ref} is a fixed value equal to 283.15 K.

In the heating mode, the following equations were used:

$$\frac{Q_h}{Q_{h,nom}} = 0.8125 - 1.6888\left(\frac{T_{L,in}}{T_{ref}}\right) + 8.6281\left(\frac{T_{S,in}}{T_{ref}}\right) - 2.8594\left(\frac{\dot{V}_L}{\dot{V}_{nom}}\right) - 3.7187\left(\frac{\dot{V}_S}{\dot{V}_{nom}}\right) \quad (5)$$

$$\frac{P_{elh}}{P_{elh,nom}} = 3.4375 + 6.1243\left(\frac{T_{L,in}}{T_{ref}}\right) + 1.4024\left(\frac{T_{S,in}}{T_{ref}}\right) - 5.3125\left(\frac{\dot{V}_L}{\dot{V}_{nom}}\right) - 5.1094\left(\frac{\dot{V}_S}{\dot{V}_{nom}}\right) \quad (6)$$

where T_{ref} is a fixed value equal to 283.15 K.

These equations are implemented in EnergyPlus tool for the energy performance evaluation of the heat pump (U.S. Department Of Energy, 2016). The coefficients of the equations have been calculated using data provided from the manufacturer and they fit the behaviour of the heat pump as a function of $T_{L,in}$, $T_{S,in,}$ V_L and V_S.

At each time step, the energy delivered and the electrical power of the heat pump were calculated considering the entering fluid temperatures and the mass flow rates of the heat carrier fluid on the source and load sides.

As above mentioned an integrated simulation simultaneously considering the building, heat pump and BHE was carried out with EnergyPlus. When the CaRM tool was used, the heat pump performance curves (Equations (3-6)), the building thermal loads, and the entering fluid temperature on the load side, calculated via EnergyPlus, were used as inputs to the model. At each calculation time step, the CaRM provided the inlet and outlet fluid temperatures on the source side and the energy efficiency of the heat pump (COP or EER respectively for the heating or cooling modes).

The simulations carried out with EnergyPlus were performed using the g-function technique to simulate the BHE. When the CaRM was utilized, the ground and the borehole heat exchangers were modelled using the following mesh parameters:

- The number of vertical subdivisions: 190 for the borehole, 4 for the surface, and 40 for the deep zones;

- The number of annular regions: 20 from the borehole axis;
- The maximum radius (r_{max}): 10 m.

At the ground level, the following parameters were considered and assumed to be constant for the entire simulation time:

- The absorptance (a): 0.7;
- The emittance (ε): 0.9;
- The specific convection thermal resistance (R_{ext}): 0.04 (m^2 K)/W.

At the ground surface, the real atmospheric conditions (air temperature and solar radiation) collected by the ARPAV weather station were utilized as the boundary conditions. At the opposite end, the value of the undisturbed ground temperature at 10 m beneath the lower end of the boreholes, i.e. at 106 m beneath the ground surface, was assumed equal to about 14 °C. The simulations were carried out with hourly time steps, just as for the weather data file.

The outlet temperature of the heat carrier fluid from the boreholes, the seasonal energy efficiency of the heat pump and the seasonal electrical energy consumption according to the different models were compared.

Results and discussion

The computer simulations made it possible to determine several parameters reflecting the behaviour of the entire building-plant system. The temperature of the heat-carrier fluid leaving the BHE, the seasonal energy performance of the heat pump (hereinafter called *S-COP* in the heating mode or *S-EER* in the cooling one) and the annual electrical consumption of the ground source heat pump according to the three different models, examined here, were compared. The *S-COP* and *S-EER* values were calculated as the ratio between the seasonal energy efficiency rate and the corresponding electrical consumption of the heat pump. Beginning with the second year, the ground source heat pump of the building was also monitored; in particular, the inlet and outlet fluid temperatures at the borehole heat exchangers were determined. The values for *Case A* (i.e. the current configuration of the boreholes) and for *Cases B* and *C* were evaluated to examine the effect of the BHE layout on the long-term thermal behaviour of the fluid temperature.

Figure 5 shows the average monthly outlet temperatures for each model for the three types of field configurations described in Table 4. The temperatures measured and recorded during real operation are also shown in Figure 5. For *Case A*, which integrates the real BHE geometry, the agreement between the experimental and simulated temperatures for the three simulation approaches is quite good over the eleven-year period (Figure 5.a). For *Cases B* and *C*, instead, the g-functions used did not reflect the real BHE geometry, and Figure 5.b-c clearly shows a worse agreement between the measured and simulated temperatures. This result confirms experimentally the risk of using g-functions that do not integrate the real BHE geometry, in particular when the layout is complex.

The actual temperature drift due to the imbalance between heating and cooling loads is well reproduced. The maximum value of the monthly average fluid temperature entering the heat pump on the ground side increased by about 10 °C during the eleven-year period (Figure 5.a). As was expected, this phenomenon is more pronounced in

the compact 4 × 4 regular grid (*Case B*); instead, Cases A and C have a similar thermal behaviour which can be noted also comparing the simulated values with the measured values in the real configuration (*Case A*).

Figure 6 outlines the temperature profiles on an hourly basis over a week in both the heating and cooling modes during the 8th simulated year, in order to highlight the differences between the simulation models. Since the assumptions used by the first two methods (i.e. g-functions) differ from the last one (i.e. CaRM), the hourly heat load can be different, thus leading to a slight difference in the simulated temperatures. The difference between *Methods 1* and *2* based on the g-functions approach using EnergyPlus is, however, negligible. As it can be seen, the outlet fluid temperature obtained by the CaRM tool is higher and lower than the other two values in the heating and cooling modes, respectively. One difference between the g-function and CaRM approaches is that the borehole thermal capacitance is not considered in *Methods 1* and *2*. In addition, CaRM considers the effect of the weahter on the ground surface whereas *Methods 1* and *2* don't take into account the heat transfer on the ground surface. These contributions are particularly evident when the heat pump is switched off; during such period, CaRM tool simulates the heat transfer between the heat-carrier fluid inside the borehole heat exchangers and the surrounding ground. In Figure 6, a higher difference between the measured and simulated values can be seen compared to the results shown in Figure 5 as the building model was calibrated on the seasonal energy load of the heat pump, considering reference control strategies and thermal loads, kept constant througout the simulation. In the reality they were subject to some changes throughout the time as it is evident during the week-end in Figure 6.b (i.e. the switch-off times of the heat pump in the evening, shown by an abrupt change of slope, are different in respect to the simulated switch-off times). A calibration on the hourly basis would require other dedicated measurements that are not available in the installed Building Management System. The difference between measured and simulated values can be due to several aspects. In fact, in all cases the effect of the horizontal coupling between the borehole heat exchangers and the heat pump was not considered in the computer simulations; moreover, the fluid temperatures were measured on board of the heat pump, therefore affected by the air temperature of the technical room when the system is swithched off.

Figure 7 shows the calculated values of the *S-COP* and *S-EER* of the heat pump for the eleven-year simulation period. Figures 7.a-b outlines the results when g-functions are calculated by GLHEPro and by the tool developed by Cimmino and Bernier (2013); Figure 7.c shows the results obtained using the CaRM tool. These values were calculated considering the entering fluid temperature at the heat pump on both the building and ground sides (Equations (3-6)) for each model. As expected the simulations demonstrate an appreciable change in the efficiency of the heat pump over the period considered: the *S-EER* value decreased over the eleven-year period due to the building's cooling dominant profile, while the *S-COP* value increased. The difference between the first and the last year in terms of the S-EER was more than 20% for all the models. This result once again highlights the importance of long-term computer simulations for GSHPs particularly when the load profile is not balanced on the ground side. The actual configuration of the boreholes (i.e. L-shape, *Case A*) and *Case C* uncover the best thermal behaviour. In *Case B* (i.e. 4 × 4 regular grid) the greatest difference was found between the first and the last year.

Figure 8 shows the annual electrical consumption of the heat pump including the constant speed pump of the ground-loop whose absorbed power is about 1800 W. In the case outlined here, the circulating pump of the ground loop is switched on when the heat pump is working. The difference between the three models, which show the same

pattern, is negligible in terms of total electrical consumption. The annual variability is due to the different climatic data that affect building loads. As it can be observed, the incidence of the circulating pump on the total electrical consumption amounts to approximately 20%.

Conclusions

Since the predefined default g-functions included in EnergyPlus' original package are unsuitable to handle the multiplicity of possible cases, a specific method to determine such functions must be adopted to achieve a reliable simulation. This study examined two methods to calculate g-functions referred to a real office building showing a multi-year ground temperature drift. The two methods, applied to the building's long-term monitoring within an EnergyPlus model, produced quite similar results when the g-functions were calculated on the real layout of the borehole filed. A third method, the CaRM, based on the numerical solution of Fourier's equation of the ground field, was also employed; it utilized the same heating and cooling load profiles calculated by EnergyPlus. The three methods produced very similar results with regard to the overall electrical energy consumption of the heat pump. The simulation results were also compared with measured values and a good agreement was found on the average monthly fluid temperature.

The only disadvantage of the CaRM tool is that the calculation process must be divided into two parts: first a simulation must be carried out to obtain the heating and cooling load profiles (not necessarily via EnergyPlus), then a simulation of the heat pump and borehole field must be performed to obtain the final result. On the other hand, the detailed numerical approach offers the opportunity of obtaining further information on the behaviour of the geothermal field, as the ground temperature at different distance from borehole axis and also along the depth. Moreover, the short-term thermal behaviour of the borehole heat exchangers can be investigated since CaRM tool considers the borehole thermal capacity, as a consequence the calculation time step can be shorter than one hour.

Nomenclature

a	Thermal diffusivity (m^2/s), surface absorptance (-)
C	Volume heat capacity (J/K)
COP	Coefficient of performance in heating mode (-)
EER	Coefficient of performance in cooling mode (-)
h_{ext}	Convection heat transfer coefficient at ground surface ($W/(m^2 K)$)
i	Ground discretization index in radial direction
j	Ground discretization index in vertical direction
L	Length (m)
L_{bore}	Borehole length (m)
q	Specific heat load (W/m)
Q	Heat rate (W)
P	Power (W)

r_{max} Radius from axis borehole beyond which the undisturbed ground is considered (m)

R Thermal resistance (K/W)

R_{ext} Convection thermal resistance at ground surface per unit area (m^2 K/W)

R_{p0} Thermal resistance between the pipe and borehole wall (m K/W)

R_{ppA} Thermal resistance between adjacent pipes (m K/W)

R_{ppB} Thermal resistance between opposite pipes (m K/W)

SCOP Seasonal coefficient of performance in heating mode (-)

SEER Seasonal coefficient of performance in cooling mode (-)

T Temperature (K)

T_{ext} External air temperature (K)

T_g Undisturbed ground temperature (K)

T_{sky} Sky temperature (K)

z Depth (m)

Greek symbols

ε Surface emittance (-)

λ Thermal conductivity (W/(m K))

τ Time (s)

Δz Length of control volume in vertical direction (m)

Subscripts

b Borehole, borehole zone, building

d Deep zone

c Cooling

el Electrical

f Fluid

g Ground

h Heating

hp Heat pump

i Inside

in Inlet

L Load side

nom Nominal

out Outlet

r Radial direction

s Surface zone

S Source side

z	Depth direction

Acknowledgements

The authors are grateful to M. Cimmino of the Ecole Polytechnique de Montréal (Canada) and to J.D. Spitler of Oklahoma State University (USA) for making the g-function softwares used in this work available to us. Special thanks are due to HiRef S.p.A. for providing the full set of performance data concerning the water to water heat pump examined in this work.

References

Al-Sallal, K.A. 2014. A Review of Buildings' Energy Challenges. International Journal of Environment and Sustainability 3(1): 42--49.

ARPAV Agenzia Regionale per la Prevenzione e per la Protezione Ambientale del Veneto. 2017. http://www.arpa.veneto.it

Cimmino, M., and M. Bernier. 2013. Preprocessor for the generation of g-functions used in the simulation of geothermal systems. Proceedings of BS2013: 13th Conference of International Building Performance Simulation Association. Chambéry, France.

Cimmino, M., M. Bernier, and F. Adams. 2013. A contribution towards the determination of g-functions using the finite line source. Applied Thermal Engineering 51(1-2): 401--412.

Cimmino, M., and M. Bernier. 2014. A semi-analytical method to generate g-functions for geothermal bore fields. International Journal of Heat and Mass Transfer 70: 641--650.

Claesson, J. and S. Javed. 2011. An analytical method to calculate borehole fluid temperatures for time-scales from minutes to decades. ASHRAE Transactions 117(2): 279--288.

Cui, P., H. Yang, and Z. Fang. 2006. Heat transfer analysis of ground heat exchangers with inclined boreholes. Applied Thermal Engineering 26(11-12): 1169--1175.

Currò Dossi, F., M. De Carli, R. Del Bianco, F. Fellin, M. Tonon, and R. Zecchin. 2003. A pilot project for a low energy building equipped with thermal slabs, heat pump and ground heat storage. 8th International IBPSA Conference Eindhoven, Netherlands, August 11--14.

De Carli, M., M. Tonon, A. Zarrella, and R. Zecchin. 2010. A computational capacity resistance model (CaRM) for vertical. Renewable Energy 35: 1537--1550.

Eskilson, P. 1987. Thermal analysis of heat extraction boreholes. Ph.D. Thesis, Lund University, Department of Mathematical Physics. Lund, Sweden.

European Parliament. 2009. Directive 2009/28/EU of the European Parliament and of the Council of 23 April 2009 on the promotion of the use of energy from renewable sources and amending and subsequently repealing Directives 2001/77/EC and 2003/30/EC. Official Journal of the European Union 140.

European Parliament. 2010. Directive 2010/31/EU of the European Parliament and of the Council of 19 May 2010 on the energy performance of buildings (recast). Official Journal of the European Union 153.

European Parliament. 2012. Directive 2012/27/EU of the European Parliament and of the Council of 25 October 2012 on energy efficiency. Official Journal of the European Union 315.

European Parliament. 2016. Directorate General for Internal Policies, Policy Department A: Economic and Scientific Policy. "Boosting Building Renovation: What potential and value for Europe?"

Gestore dei Servizi Energetici GSE. 2017. Rapporto Statistico – Energia da fonti rinnovabili in Italia 2015. Text available on GSE website at www.gse.it.

IEA International Energy Agency. 2011. Technology Roadmap – Energy-efficient Buildings: Heating and Cooling Equipment (2011). Text available on IEA website at www.iea.org.

IEA International Energy Agency. 2016. Energy Efficiency Market Report 2016. Text available on IEA website at www.iea.org.

Kollet, S., Cvijanovic, I., Schüttemeyer, D., Moene, A.F., and P. Bayer, 2009. Influence of the Sensible Heat of Rain, Subsurface Heat Convection and the Lower Temperature Boundary Condition on the Energy Balance at the Land Surface. Vadose Zone Journal 8(4): 1--13.

Kusuda, T. 1976. NBSLD, the Computer Program for Heating and Cooling Loads in Buildings. National Bureau of Standards Building Science Series 69.

Lamarche, L., and B. Beauchamp. 2007. A new contribution to the finite line-source model for geothermal boreholes. Energy and Buildings 39(2): 188--198.

Lamarche, L. 2011. Analytical g-function for inclined boreholes in ground-source heat pump systems. Geothermics 40(4): 241--249.

Lamarche, L. 2017. Mixed arrangement of multiple input-output borehole systems. Applied Thermal Engineering 124: 466--476.

Lazzarotto, A. 2014. A network-based methodology for the simulation of borehole heat storage systems. Renewable Energy 62: 265--275.

Lazzarotto, A. 2016. A methodology for the calculation of response functions for geothermal fields with arbitrarily oriented boreholes: Part 1. Renewable Energy 86: 1380--1393.

Lazzarotto, A., and F. Björk. 2016. A methodology for the calculation of response functions for geothermal fields with arbitrarily oriented boreholes: Part 2. Renewable Energy 86: 1353--1361.

Luo, J., J. Rohn, M. Bayer, A. Priess, and W. Xiang. 2014. Analysis on performance of boreholeheat exchanger in a layered subsurface. Applied Energy 123: 55–65.

Marcotte, D. and P. Pasquier. 2009. The effect of borehole inclination on fluid and ground temperature for GLHE systems. Geothermics 38(4): 392--398

Marcotte, D., P. Pasquier, F. Sheriff, and M. Bernier. 2010. The importance of axial effects for borehole design of geothermal heat-pump systems. Renewable Energy 35(4): 763--770.

Marcotte, D., and P. Pasquier. 2014. Unit-response function for ground heat exchanger with parallel, series or mixed borehole arrangement. Renewable Energy 68: 14--24.

Pasquier, P., and D. Marcotte. 2014. Joint use of quasi-3D response model and spectral method to simulate borehole heat exchanger. Geothermics 51: 281--299.

Priarone, A., Fossa, M. 2016. Temperature response factors at different boundary conditions for modelling the single borehole heat exchanger. Applied Thermal Engineering 103: 934–44.

Rivera, J.A., Blum, P., Bayer, P. 2016 a. A finite line source model with Cauchy-type top boundary conditions for simulating near surface effects on borehole heat exchangers, – Energy, 98, 50–63.

Rivera, J.A., Blum, P., Bayer, P. 2016b. Influence of spatially variable ground heat flux on closed-loop geothermal systems: Line source model with nonhomogeneous Cauchy-type top boundary conditions. – Applied Energy, 180, 572--585.

Rivera, J.A., Blum, P., Bayer, P. 2017. Increased ground temperatures in urban areas: Estimation of the technical geothermal potential. – Renewable Energy, 103, 388--400.

Ruiz-Calvo, F., De Rosa, M., Monzó, P., Montagud, C., Corberán, JM. 2016. Coupling short-term (B2G model) and long-term (g-function) models for ground source heat exchanger simulation in TRNSYS. Application in a real installation. Applied Thermal Engineering 102: 720–32.

Sorrell, S. 2015. Reducing energy demand: A review of issues, challenges and approaches. Renewable and Sustainable Energy Reviews 47: 74--82.

Spitler, J.D. 2000. GLHEPRO a design tool for commercial building ground loop heat exchangers. In: Proceedings of fourth international heat pumps in cold climates conference. Aylmer, Quebec; 17th – 18th August.

Stephenson, D. G., and G.P. Mitalas. 1967. Cooling load calculations by thermal response factor method. ASHRAE Transactions 73, Part I: III.1.1-III.1.7.

Ürge-Vorsatz, D., L.F. Cabeza, S. Serrano, C. Barreneche, and K. Petrichenko. 2015. Heating and cooling energy trends and drivers in buildings. Renewable and Sustainable Energy Reviews 41: 85--98.

U.S. Department Of Energy. 2016. Engineering Reference Manual. In EnergyPlus V8.5.

U.S. Green Building Council. 2017. https://new.usgbc.org/ (Access: November 2017)

Xu, X., and J.D. Spitler. 2006. Modeling of Vertical Ground Loop Heat Exchangers with Variable Convective Resistance and Thermal Mass of the Fluid. Proceedings of the 10th international conference on thermal energy storage. Pomona NJ.

Yavuzturk, C., J.D. Spitler, and S.J. Rees. 1999. A Transient Two-dimensional Finite Volume Model for the Simulation of Vertical U-tube Ground Heat Exchangers. ASHRAE Transactions 105(2): 465--474.

Zarrella, A., A. Capozza, and M. De Carli. 2013 a. Analysis of short helical and double U-tube borehole heat exchangers: A simulation-based comparison. Applied Energy 112: 358--370.

Zarrella, A., A. Capozza, and M. De Carli. 2013b. Performance analysis of short helical borehole heat exchangers via integrated modelling of a borefield and a heat pump: A case study. Applied Thermal Engineering 61: 36--47.

Zarrella, A., and P. Pasquier. 2015. Effect of axial heat transfer and atmospheric conditions on the energy performance of GSHP systems: A simulation-based analysis. Applied Thermal Engineering 78:591-604.

Zarrella, A., G. Emmi, R. Zecchin, and M. De Carli. 2017. An appropriate use of the thermal response test for the design of energy foundation piles with U-tube circuits. Energy and Buildings 134: 259--270.

Zeng, H.Y., N.R. Diao, and Z.H. Fang. 2002. A finite line-source model for boreholes in geothermal heat exchangers. Heat Transfer Asian Research 31(7): 558–67.

Table 1 – Nominal parameters of the heat pump.

		Heating	**Cooling**
Thermal capacity	[kW]	97.0	111.0
COP / EER	[-]	4.60	5.98
Temperatures of the heat-carrier fluid on the ground side (inlet/outlet at the heat pump)	[°C]	8/5	25/30
Temperatures of the heat-carrier fluid on the building side (inlet/outlet at the heat pump)	[°C]	31/35	19/15
Mass flow rate on the ground side	[kg/s]	5.56	5.56

Table 2 – Thermal transmittance of the building's envelope.

	[W/(m^{2}K)]
External Wall – West Side	0.45
Ground Contact Wall	0.49
External Wall – East Side	0.18
Roof	0.57
Ground Contact Floor	0.33
Glazed Facade – Nord Side	1.86
Double Skin Facade – South Side	1.30
Skylight – East Side	1.45

Table 3 – Characteristics of the building's internal spaces

Zone	Number of zones	Floor Surface [m^2]	Lighting [W/m^2]	Occupancy [$People/m^2$]	Electric equipment [W/m^2]
Auditorium	1	114.2	39.40	0.53	-
Break Room	1	18.32	11.35	0.33	-
Corridor	10	219.49	7.75	-	-
Front-Office	1	33.62	8.33	0.03	2.68
Library	1	51.6	8.68	-	-
Lobby	3	518.24	2.84	-	-
Mechanical Room	4	74.35	8.42	-	94.15
Meeting Room	6	153.11	9.69	0.15	4.70
Office	14	293.52	10.49	0.08	7.36
OpenSpace	6	771.95	9.25	0.08	7.46
Printers Room	3	38.26	4.39	-	39.21
Storage	3	144.58	12.44	-	-
Toilette	6	83.28	12.85	-	-

Table 4 – The three simulations.

	Pattern of the borehole field	Spacing [m]	Number of Boreholes \ Total borehole length [m]	Notes
Case A	L – shape	7	16 \ 1520	Real Configuration
Case B	4 × 4 Grid	7	16 \ 1520	-
Case C	U – shape	7	16 \ 1520	-

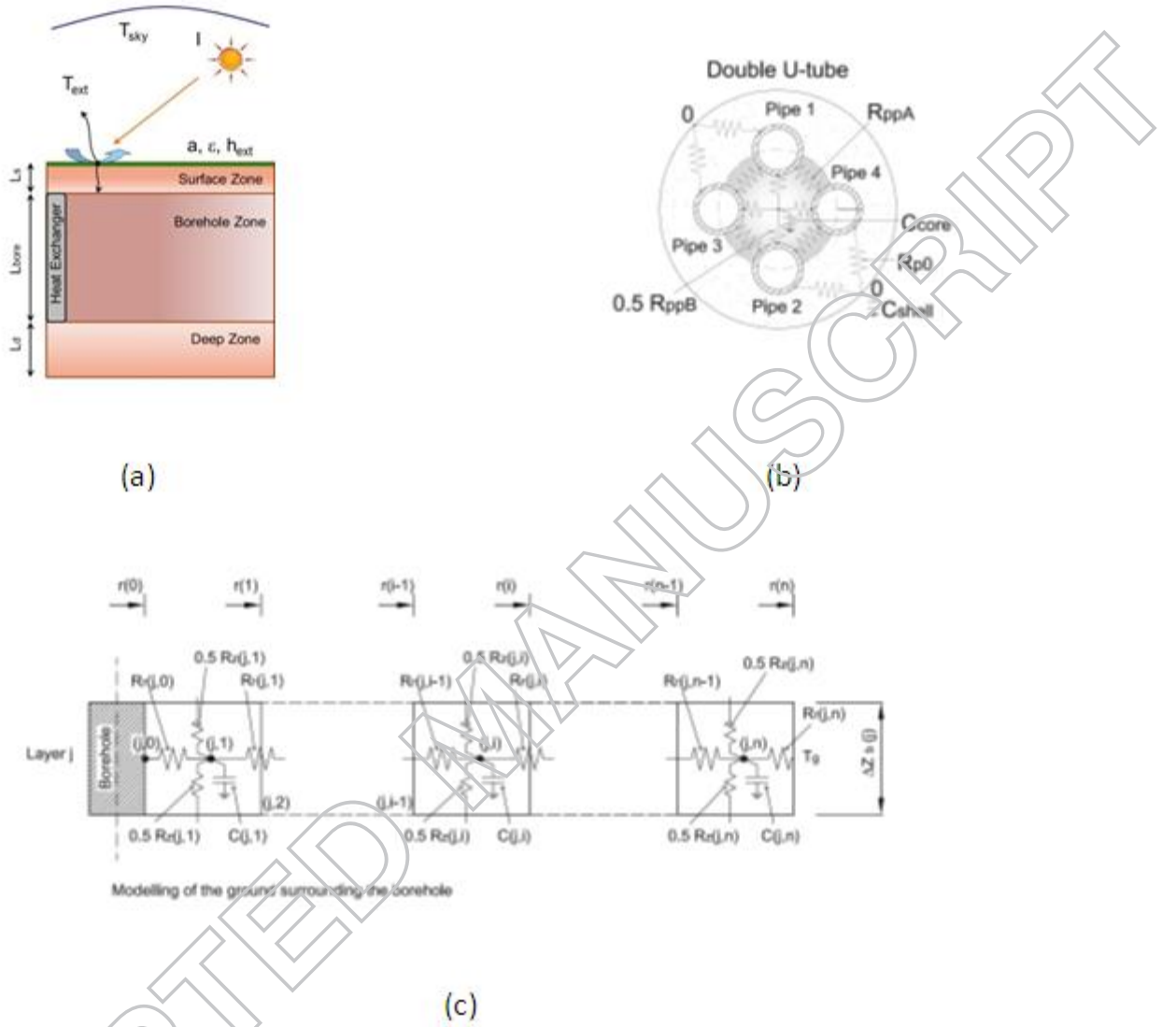

Figure 1 – Outline of the CaRM's modelling approach.

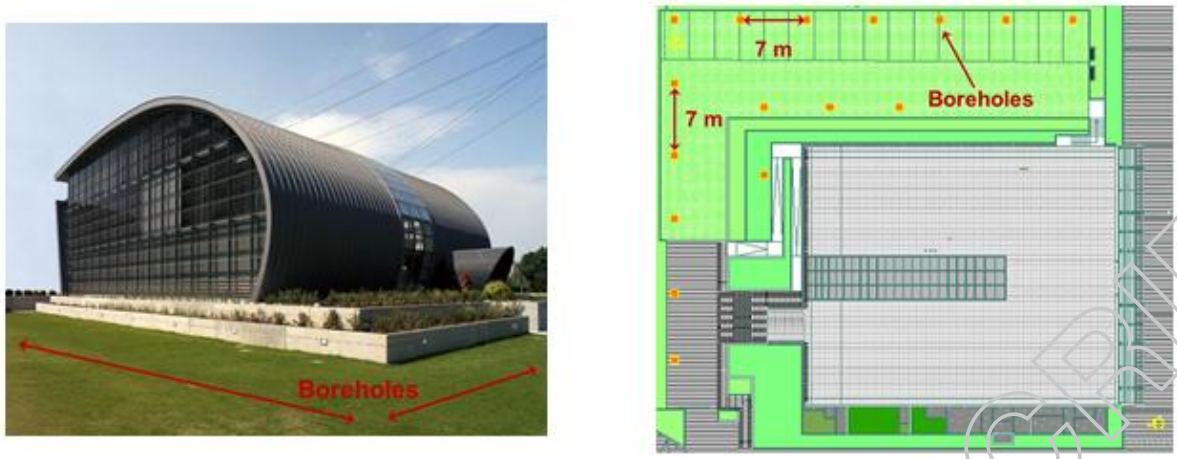

(a) (b)

Figure 2 – South-East view of the building (a) and the arrangement of the boreholes positioned around the building (b).

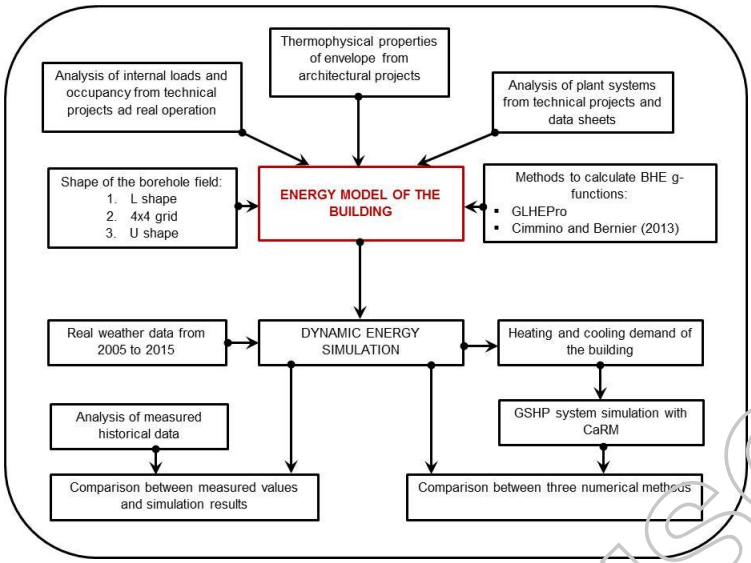

Figure 3 – Approach for the computer simulations.

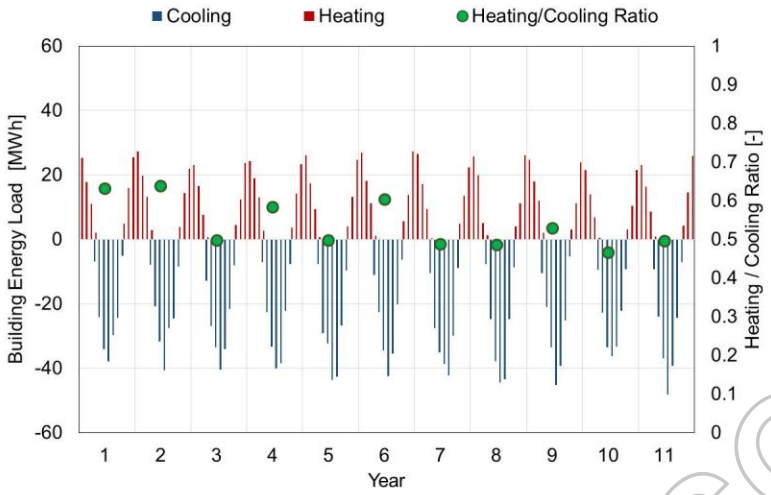

Figure 4 – Synthesis of the building's monthly load profile derived from hourly calculations.

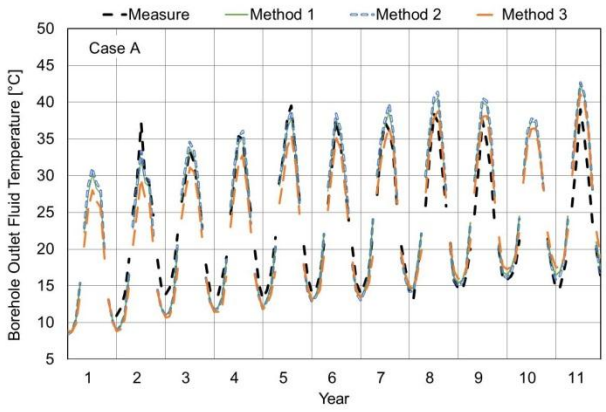

(a)

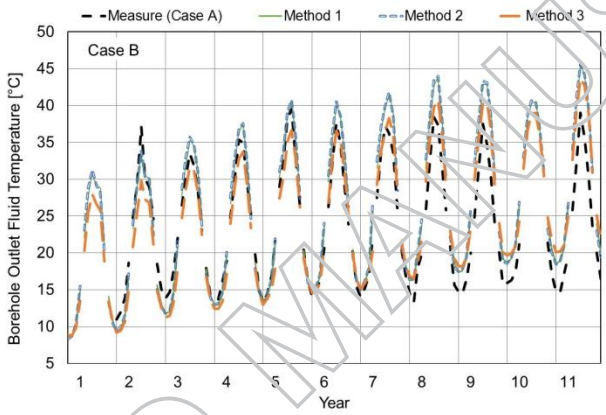

(b)

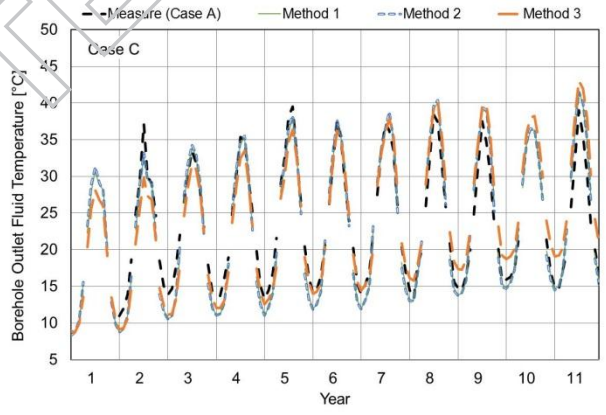

(c)

Figure 5 – Average monthly fluid temperatures leaving the boreholes for the L-shape (real) (a), grid 4×4 (b) and U-shape (c) configurations.

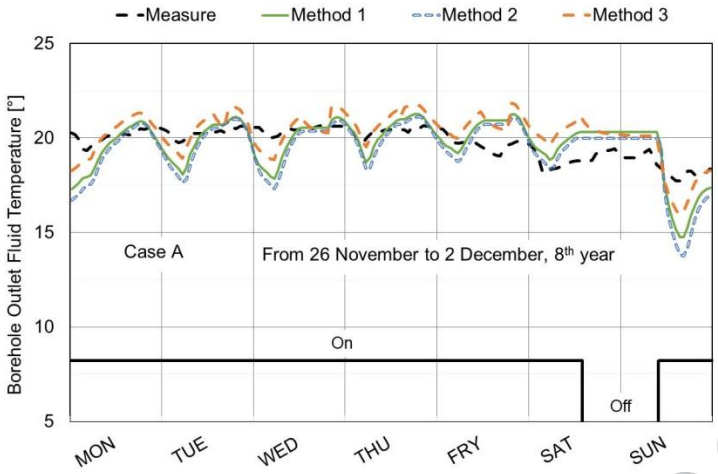

(a)

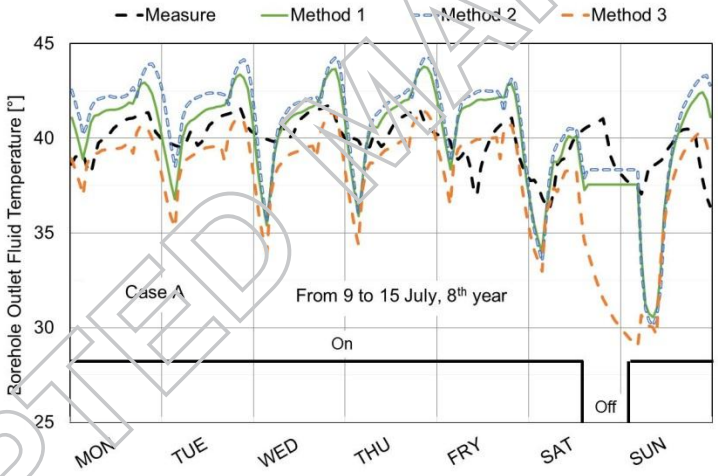

(b)

Figure 6 – Hourly temperature profiles of the fluid leaving the boreholes for Case A (L-shape) for one week: (a) in the winter and (b) in the summer during the 8th year.

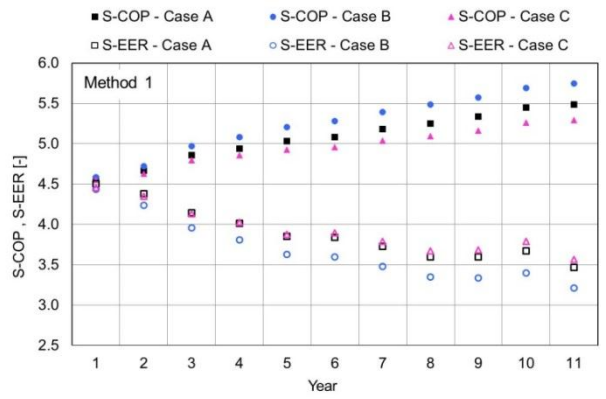

(a)

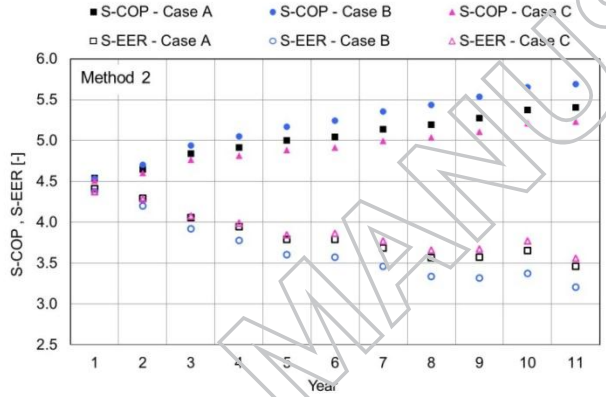

(b)

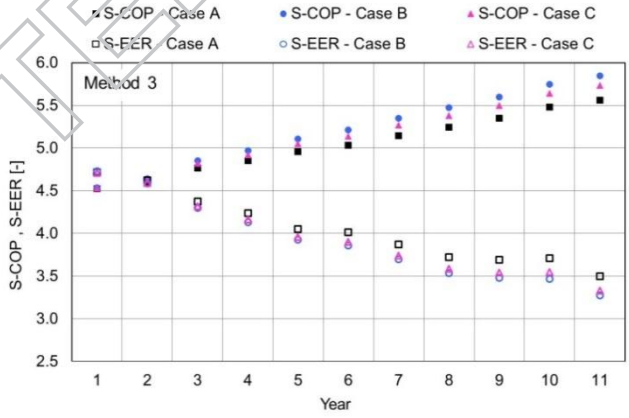

(c)

Figure 7 – Monthly heat pump efficiency calculated for simulation method 1 (a), Method 2 (b) and Method 3 (c) for the three field configurations.

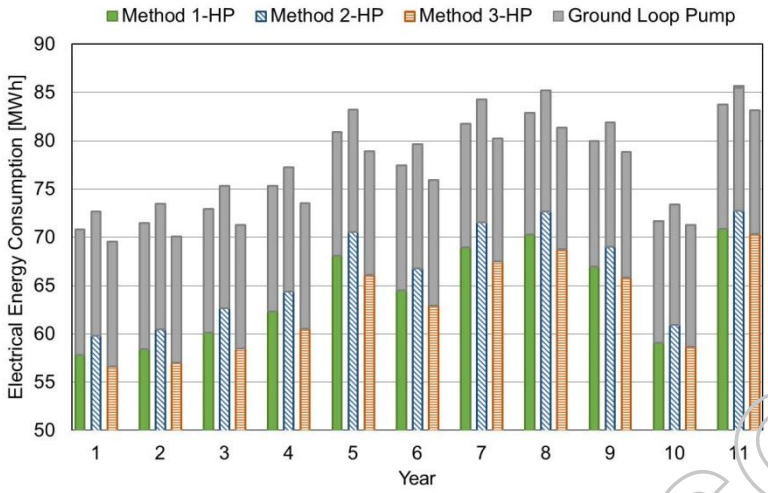

Figure 8 –Annual electrical energy consumption of the heat pump and ground loop pump, referred to the real configuration.